Journal of Medicinal Chemistry

ARTICLE

pubs.acs.org/jmc

Binding Inhibitors of the Bacterial Sliding Clamp by Design†

Gene Wijffels,[*,‡] Wynona M. Johnson,[§] Aaron J. Oakley,[∥,⊥] Kathleen Turner,[§] V. Chandana Epa,[#] Susan J. Briscoe,[‡] Mitchell Polley,[§] Andris J. Liepa,[§] Albert Hofmann,[§] Jens Buchardt,[▽,◆] Caspar Christensen,[▽,◆] Pavel Prosselkov,[∥,¶] Brian P. Dalrymple,[‡] Paul F. Alewood,[▽] Philip A. Jennings,[‡,+] Nicholas E. Dixon,[∥,⊥] and David A. Winkler[§,○]

[‡]CSIRO Livestock Industries, 306 Carmody Road, St. Lucia, Queensland 4067, Australia

[§]CSIRO Material Science and Engineering, Bayview Avenue, Clayton, Victoria 3168, Australia

[∥]Research School of Chemistry, Australian National University, Canberra, Australian Capital Territory 0200, Australia

[⊥]School of Chemistry, University of Wollongong, New South Wales 2522, Australia

[#]CSIRO Material Science and Engineering, 343 Royal Parade, Parkville, Victoria 3052, Australia

[▽]Institute of Molecular Bioscience, 306 Carmody Road, University of Queensland, St. Lucia, Queensland 4067, Australia

[○]Monash Institute for Pharmaceutical Sciences, 381 Royal Parade, Parkville, Victoria 3052, Australia

Supporting Information

ABSTRACT: The bacterial replisome is a target for the development of new antibiotics to combat drug resistant strains. The β_2 sliding clamp is an essential component of the replicative machinery, providing a platform for recruitment and function of other replisomal components and ensuring polymerase processivity during DNA replication and repair. A single binding region of the clamp is utilized by its binding partners, which all contain conserved binding motifs. The C-terminal Leu and Phe residues of these motifs are integral to the binding interaction. We acquired three-dimensional structural information on the binding site in β_2 by a study of the binding of modified peptides. Development of a three-dimensional pharmacophore based on the C-terminal dipeptide of the motif enabled identification of compounds that on further development inhibited $\alpha-\beta_2$ interaction at low micromolar concentrations. We report the crystal structure of the complex containing one of these inhibitors, a biphenyl oxime, bound to β_2, as a starting point for further inhibitor design.

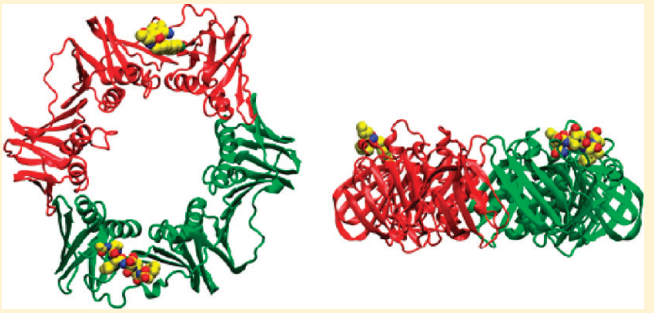

INTRODUCTION

The bacterial replisome is a clear but underexploited target for the development of new classes of antibiotics to address the problem of drug resistance.[1,2] The complex multiprotein machinery of the bacterial DNA replication and repair systems offer many target sites for the intervention of drugs to ameliorate or arrest the progress of infectious disease.[2,3] Indeed, the bacterial replicative polymerases and even the complete replisome have been the targets of recent drug screening and structure−function studies in the search for new antimicrobial leads.[2−6]

A highly conserved component of the bacterial replisome is the sliding clamp, a homodimer of two β subunits that form a stable donut shaped ring around DNA,[7,8] tethering the replicative machinery while allowing the complex to slide along the duplex.[9] The clamp hosts each of the DNA polymerases (Pol I−V) that function in chromosomal DNA replication and repair,[10,11] and also interacts directly with the δ subunit of clamp loader complex,[12] with Hda, a protein involved in initiation of replication,[13] and several other proteins that function in DNA replication and repair.[14,15] The essential and central role of the clamp, the conservation of its interactions with many partners, and its limited cellular availability of 300−600 β_2 dimers per cell[16,17] make it an attractive target for rational design of new antimicrobial agents.[1,2,5]

Bioinformatic analysis identified a conserved clamp binding site, a C-terminal or proximal C-terminal pentameric motif, QL[S/D]LF, within the sequences of DNA polymerases of many bacteria.[18] Experimental evidence substantiated that peptides bearing the consensus clamp binding motif (CBM) or related hexapeptide sequences bind directly to the clamp and compete successfully with clamp binding proteins.[18,19] Mutation of the first-identified (internal) CBM in the *Escherichia coli* Pol III α polymerase subunit with various versions of the motif significantly affected Pol III function *in vitro* and *in vivo*.[20]

Received: April 12, 2011
Published: May 23, 2011

An alternative region of the α subunit (of the *E. coli* Pol III replisome), located very close to its C-terminus, had earlier been proposed to be the more critical clamp-binding site.[21] A peptide bearing this sequence, QVELEFD, did indeed compete successfully in clamp binding and interfere in DNA replication assays. Nevertheless, Dohrmann and McHenry[20] demonstrated that the internal α subunit site, QADMF, is absolutely required by Pol III holoenzyme for processive DNA synthesis. The precise roles of the two CBMs in the Pol III α subunit remain to be fully elucidated.

Crystal structures of complexes of CBM peptides from Pols II, III (C-terminal site) and IV bound to β_2 are now available.[5,22,23] The peptides occupy the same surface pocket comprising two subsites. In simple terms, subsite 1 is an 8.5 Å deep square pocket that accommodates the C-terminal Leu-Phe (in pentapeptides) or Leu-Xaa-Phe (in hexapeptides) portion of the motif. Subsite 2 is a narrow shallow slot (4.5 Å deep) that is occupied by the N-terminal portion of the CBM.[5,22,23]

In a search for small molecule binders of the sliding clamp, the O'Donnell group[5] screened a library of 30,600 small synthetic molecules and successfully identified a lead entity, **1** (RU7[5]). This compound inhibited *in vitro* DNA synthesis by Pol III and also competed with a peptide containing the *Streptococcus pyogenes* Pol C CBM for binding to *S. pyogenes* β_2.[5] A cocrystal structure of **1** with the clamp revealed that it was bound only within the deeper subsite 1 and with fewer contacts than the larger synthetic peptides.[5]

With limited structural information available at the time we commenced this study, we adopted the alternate strategy of rational molecular design. This required assembly of three-dimensional (3D) spatial information about the target site through interrogation with competitive binders (ligand based design) and/or protein crystal structures (receptor structure based design). We anticipated that a combination of these approaches would lead to an informed design process.

To build up a 3D model through ligand interrogation, we generated a series of synthetic pentapeptides incorporating natural and non-natural substitutions of the C-terminal LF component of the CBM. Assessment of these as inhibitors in binding assays led to an optimized peptide. Since modifications of LF gave improved binding, we developed a novel 3D informatic technique to define a pharmacophore query based on the likely conformations of the [$^S/_D$]LF moiety. Searches of databases of small synthetic compounds with this 3D motif identified a small number of hits that showed weak inhibitory activity. A group of small molecules with related structures were then selected for confirmation of binding, and those with improved binding were used for cocrystallization with *E. coli* β_2.

We now report the structure of a new small chemical entity thus identified, bound in the CBM binding site of β_2. We compare it to the binding of **1** in the same site and a model of binding of the optimized pentapeptide. Together, the structural information from these sources allows inference of ligand design modifications that may be expected to provide compounds with improved binding to β_2.

RESULTS AND DISCUSSION

SAR of Modifications to the Peptide Motif. Synthetic peptides with different CBMs generally exhibit correlated inhibitory activities (IC_{50}) in a simple α−β_2 plate binding assay and a β_2−consensus CBM surface plasmon resonance (SPR) competition assay.[19] Where available, the dissociation constants (K_D) of peptide−β_2 complexes measured directly by surface plasmon resonance (SPR) also concur with their inhibitory activities.[19] Since the Leu_4-Phe_5 portion of the consensus pentameric CBM (QL[$^S/_D$]LF) is buried deeply in subsite 1,[5,22,23] we anticipated that changes in these residues would have significant potential for optimization.

Table 1. Inhibition of α−β_2 and β_2−Consensus Peptide Assays by Peptide Variants

peptide sequence	α−β_2 binding IC_{50} (nM)[a]	SPR IC_{50} (nM)[a]
DnaE Nonomer Peptides with Substitutions at Positions 4 and 5 of the DnaE CBM, QADMF		
IG QLSLF GV	2,300 ± 1,100	550
IG QADMF GV	96,000	3,000[b]
IG QADLF GV	56,000	nd
IG QADIF GV	315,000	nd
IG QADFF GV	174,000	nd
IG QADWF GV	345,000	nd
IG QADMW GV	282,000	nd
N-Acetylation of the Pentameric CBM, QLDLF		
QLDLF	2,600 ± 1,400	620
pyroQLDLF	4,500 ± 700	nd
Ac-QLDLF	70 ± 20	400
Most Competitive Peptides with Substitution in Positions 4 and 5 of Ac-QLDLF		
Ac-QLDL[2ClF]	34 ± 8	117 ± 49
Ac-QLDL[3ClF]	11 ± 1	49 ± 8
Ac-QLDL[4ClF]	27 ± 18	20 ± 5
Ac-QLDL[3,4ClF]	21 ± 6	23 ± 11
Ac-QLDM[3,4ClF]	37 ± 1	33 ± 1
N-Terminal Extensions to QLDL[3,4ClF]		
propionyl-	63 ± 11	61 ± 17
pivaloyl-	62 ± 19	69 ± 23
benzyloxyacetyl-	67 ± 17	337 ± 18
3-indoleacetyl-	66 ± 7	537 ± 76
2,4-dimethoxybenzoyl-	42 ± 15	27 ± 2
benzoyl-	69 ± 24	456 ± 80
isobutyloxycarbonyl-	20 ± 15	41 ± 21
methyloxycarbonyl-	86 ± 0.5	89 ± 10

[a] Assayed as described.[19] IC_{50} values represent the concentration of peptide required to inhibit interactions by 50%. Mean ± SEM of at least 2 independent measurements. nd, not done. [b] Data from Wijffels et al.[19]

A series of substitutions were made within the context of pepDnaE-n (IGQADMFGV).[19] This peptide with $Q_1A_2D_3M_4F_5$ as its CBM exhibited a moderate K_D (SPR) and modest IC_{50} in the α−β_2 plate binding assays relative to those of peptides containing the consensus sequence.[19] Consistent with previous studies, substitution of Met_4 with Leu improved inhibitory activity in the α−β_2 and SPR assays (Table 1). Peptides with Ile, Phe, and Trp in position 4 or Trp in position 5 were weak inhibitors in the plate assays. Substitutions with Cys, Val, or Tyr at position 4 or Cys, Leu, Ile, Val, or Tyr at position 5 abolished inhibitory activities (not shown).

The observation that the β_2 binding site tolerates some amino acids with bulky but neutrally charged (lipophilic) side chains led

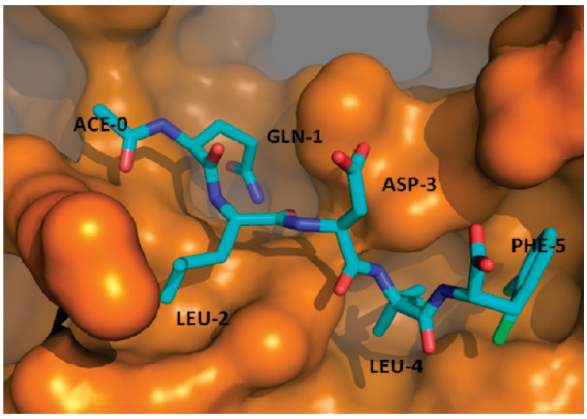

Figure 1. Computational model for the complex between β (in orange surface representation) and the peptide Ac-QLDL[3,4ClF] in stick representation.

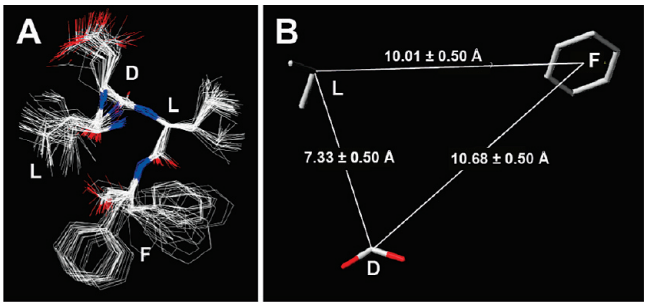

Figure 2. (A) Consensus superimposition of examples of LDLF motifs from the PDB. (B) 3D pharmacophore query for the dominant DLF conformation. The vertex points represent the terminal side chain moieties of D (carboxyl carbon), L (dimethyl), and F (phenyl ring centroid).

us to seek increased structural diversity by substitution of positions 4 and 5 with large non-natural side chains and ring structures. This study was conducted using the N-terminally acetylated pentamer, Ac-$Q_1L_2D_3L_4F_5$. The unprotected peptide was found to be susceptible to spontaneous cyclization of the N-terminal Gln to pyroglutamine, and this was a concern as the pyroGln pentamer was a less effective inhibitor in the $\alpha-\beta_2$ plate assay (Table 1). However, in a serendipitous finding, acetylation of the N-terminus by itself caused a 40-fold decrease in the $\alpha-\beta_2$ IC_{50} from 2.6 μM to 70 nM. Thus, a series of peptides based on Ac-QLDLF were prepared where Phe_5 was replaced by substituted phenylalanines, a benzylalanine, naphthylalanines, or pyridylalanines. Assay of these peptides revealed that those with chlorinated phenylalanines were superior, with a 3−7-fold improvement in the $\alpha-\beta_2$ inhibitory activity relative to that of the parent peptide Ac-QLDLF (Table 1 and Table S1, Supporting Information).

In the next iteration, a series of peptides with substitutions of non-natural amino acids at position 4 of Ac-QLDL[3,4ClF] (3,4ClF = 3,4-dichloro-Phe) were studied. Only the methionine substituted pentamer was competitive. The 2- and 3-chloro-Phe, methyl-leucine, 3-allylglycine, and cyclohexylalanine derivatives retained various levels of inhibitory activity (with $\alpha-\beta_2$ IC_{50} values of 0.1−0.6 μM; Table S2, Supporting Information). Thus, in the context of a 3,4-dichloro-Phe_5, there appeared to be limited scope to enhance activity with modifications at position 4.

The improved inhibitory activity of the N-acetylated pentamer also encouraged further investigation of substitution at the N-terminus (Table S3, Supporting Information). A series of aliphatic and aromatic amides, carbamates, and sulphonamides were tested as N-terminal derivatives of QLDL[3,4ClF] (Table 1). The best inhibitors contained the aliphatic amide functionality, where linear and cyclic groups were well tolerated in the $\alpha-\beta_2$ assay. Two aromatic amides, benzoyl and 2,4-dimethyl benzoyl, were also good inhibitors, as were the simple isobutyl- and methyl carbamates. None of the sulphonamides were inhibitory (Table S3, Supporting Information).

Good inhibitory activity in the plate binding assay was not consistently paralleled by competitive performance in the SPR assay. The presence of large ring structures markedly increased the SPR IC_{50}, the one exception being the 2,4-dimethylbenzoyl substituent. From a design viewpoint, it is clear that incorporation of N-terminal extensions of the peptide that project from subsite 2 does not always impact peptide binding.

Modeling of Non-Natural Substitutions at Position 5 of the Pentameric CBM. With the availability of experimentally determined structures of β_2 bound to various peptide and protein ligands,[5,22,23] we modeled the structure of its complex with peptide Ac-QLDL[3,4ClF] (Figure 1). The model indicated that β residues Arg152, Thr172, Gly174 to Leu177, Pro242, Val247, Tyr323, Val344, Ser346, Val360, and Met362 to Arg365 interact with the peptide. Leu_2, Leu_4, and $[3,4\text{-dichloro-Phe}]_5$ of the peptide are all situated in the hydrophobic subsites in β; the 3,4-dichloro-Phe contacts residues Thr172, Leu177, Pro242, and Val247 of subsite 1.

The model is fully consistent with the experimental data. Chlorine substitution at the 3- and 4-positions of the Phe_5 ring produces better van der Waals' contacts and stronger hydrophobic interactions, consistent with the lower IC_{50} value (Table 1). Subsite 1 is not large enough to accommodate benzyl, biphenyl, or naphthalene moieties. Hence, peptides where Phe_5 is substituted with these groups exhibited weaker interactions with β. While a pyridine could be accommodated in the pocket as easily as a phenyl ring, it would have a larger desolvation energy penalty on transfer from water to the hydrophobic protein environment. This would explain the higher IC_{50} values observed when the phenyl ring is substituted by pyridine. The *N*-acetyl substituent of Gln_1 (labeled as ACE-0 in Figure 1) interacts favorably with β, forming a hydrogen bond with the backbone of Arg365, accounting for the significant increase in binding affinity upon N-acetylation (Table 1). Because of the space around the *N*-acetyl group, larger N-terminal amides can be accommodated without affecting interaction with β (Table 1). However, replacement of the *N*-acetyl group with bulky sulfonyl groups (Table S3, Supporting Information) has an adverse effect on this favorable interaction due to the change in geometry (tetrahedral sulfonyl cf. the planar amide group) and steric clashes.

Conserved Tertiary Structure in the Peptide Motif. The peptide study indicated scope for improvement of binding through modifications of the Leu_4-Phe_5 moiety of the CBM. We next investigated structural conservation of $[^D/_S]$LF motifs, mindful that in simple binding assays the linear tripeptides alone were poor inhibitors.[18] We extracted from the PDB all occurrences of the LDLF sequence in proteins whose structure had been determined to better than 3 Å resolution. Of the 122 examples found, 85 LDLF segments (70%) adopted a similar conformation (Figure 2A). Two populations of Phe_5

dx.doi.org/10.1021/jm2004333 |J. Med. Chem. 2011, 54, 4831–4838

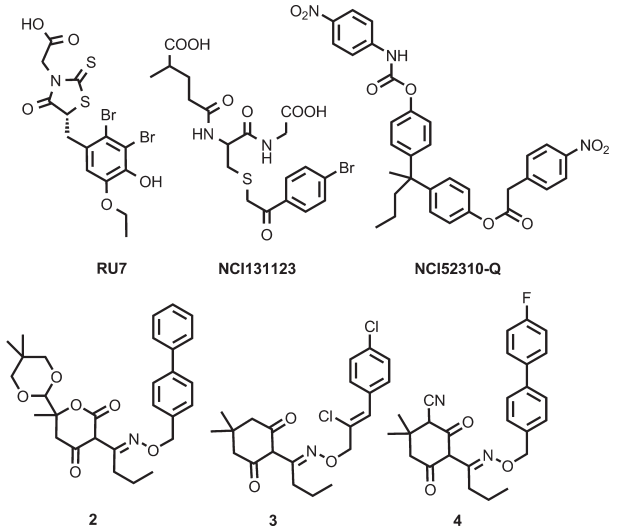

Figure 3. Structures of small molecule mimics of the DLF component of the CBM.

conformations was the dominant variation among these structures, while the Asp and Leu side chains occupied relatively restricted regions of conformational space.

Virtual Screening for Small Molecule Tripeptide Motif Mimetics. By choosing average structures representative of each of the two dominant Phe_5 conformations, 3D pharmacophore queries could be generated for each; Figure 2B shows a pharmacophore query for the DLF peptide motif. These pharmacophores were used to conduct 3D flexible database searches in the National Cancer Institute (NCI) and in-house chemical databases. The NCI database[24] search generated several hits that matched the query that did not contain significant additional structural features that may interfere with binding to β_2. Two compounds (of 25 tested) showed weak inhibitory activity in the $\alpha-\beta_2$ assay: NCI 131123 and NCI 52310-Q (Figure 3) had $\alpha-\beta_2$ IC_{50} values of 210 and 300 μM, respectively.

A similar virtual screen was conducted on the in-house collection of 32,000 compounds, followed by an $\alpha-\beta_2$ plate binding assay of 20 virtual hits. Two compounds, **2** ($\alpha-\beta_2$ IC_{50} = 270 μM) and **3** (350 μM), showed consistent, albeit weak, inhibition. Significantly, both compounds (Figure 3) were of related oximinodioxo-cyclohexane and -pyran chemical classes.

Structure of β_2 with a Bound Small Molecule Peptide Motif Mimic. Assay of 155 analogues of these oxime ether hits indicated that $\alpha-\beta_2$ binding inhibition was characteristic of these classes (details to be reported elsewhere).

Crystallization trials on a subset of oximinodioxo-cyclohexane and -pyran peptide mimetics that exhibited superior inhibitory activity resulted in the successful cocrystallization of biphenyloxime ether **4** with *E. coli* β_2. This compound exhibited an $\alpha-\beta_2$ IC_{50} of 40 $\pm$ 17 μM (7 replicates) and an SPR IC_{50} of 8.3 μM (2 replicates). The initial electron density maps calculated from the X-ray diffraction data at 1.9 Å resolution showed positive electron density in the CBM binding region of each β monomer (peaks >6σ in the $mF_o - DF_c$ electron density map). This was easily interpreted as compound **4**. After several rounds of model building and refinement, the final model consisted of a β_2 dimer with one molecule of **4** in each CBM binding site. Statistics pertaining to the X-ray structure and model are given in Table S4 (Supporting Information). The final R and R_{free} values are

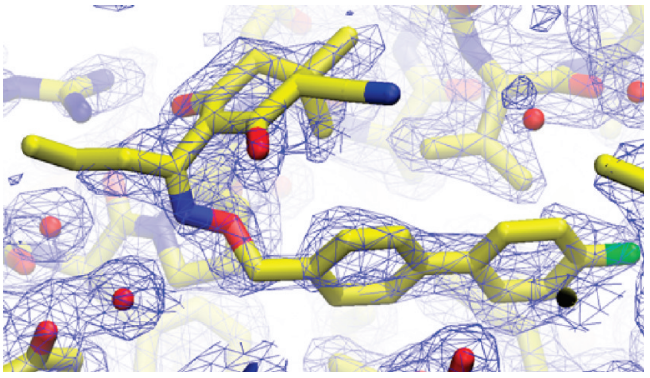

Figure 4. Compound **4** bound in the CBM binding site of the *E. coli* β_2 sliding clamp. The $2mF_o - DF_c$ electron density omit-map is drawn in "wire basket" form, contoured at 0.33 e/Å^3 (1σ). Carbon atoms are in yellow, and water molecules are shown as red spheres.

somewhat higher than expected for a structure at 1.9 Å resolution, most likely due to twinning of the crystal. Nevertheless, the final electron density for the protein and ligand is excellent (Figure 4).

Overall, the structures of ligand free[25] and ligand bound forms of the sliding clamp are very similar, superimposing with an rmsd of 1.3 Å over all 732 Cα atoms. There is a slight change in the overall shape of the β_2 ring. However, this may reflect the effects of crystal packing rather than ligand binding. The X-ray data revealed that **4** is bound in a hydrophobic cleft on the surface of both β monomers (see Figure 4). This pocket is formed by Arg152, Tyr154, Gly174, Pro242, Val247, Val360, and Met362 (nominally subsite 1). The biphenyl group of **4** participates in hydrophobic interactions with the pocket, and the distal aromatic ring in **4** is twisted out of the plane of the proximal ring. The cyano group fits into a small hydrophobic pocket that would not accommodate a larger ligand. This single hydrophobic interaction at this end of the molecule may account for the improved binding of this compound as compared to that of **2** and **3**. The conformations of the oxime link and propyl side chains are different in the ligands bound to each monomer (Figure 5C). Curiously, a single hydrogen bond is evident between one carbonyl oxygen and Arg240 in one β monomer but not in the other. Potentially Arg152 could twist around to form a hydrogen bond with the other carbonyl, but it does not. These observations are not surprising when one considers that the cyclohexanedione portion of the ligand is predominantly exposed to the solvent and that there may be little energetic advantage in the formation of a hydrogen bond between the ligand and the protein as compared to the solvent.

By superimposing the structure of ligand free β_2 with the above structure, it is possible to determine which residues have moved upon the binding of **4**. The most dramatic movement is seen in Met362, which is partly disordered in the ligand free structure. In the complex, the Met362 side chain lies above one of the biphenyl rings. There are also compensatory movements in Val247, Pro242, and Arg152, which have moved toward the biphenyl system of **4**.

The structure of the β_2 complex with **4** can be compared with the complex with **1**,[5] a small-molecule compound that selectively inhibits Pol III. Compound **1** features a dibrominated aromatic ring that overlaps with the fluorobiphenyl group of **4** (Figure 6A). Both make hydrophobic interactions with Leu177, Val247, Val360, and Met362 in subsite 1. The aromatic groups of both

dx.doi.org/10.1021/jm2004333 |J. Med. Chem. 2011, 54, 4831–4838

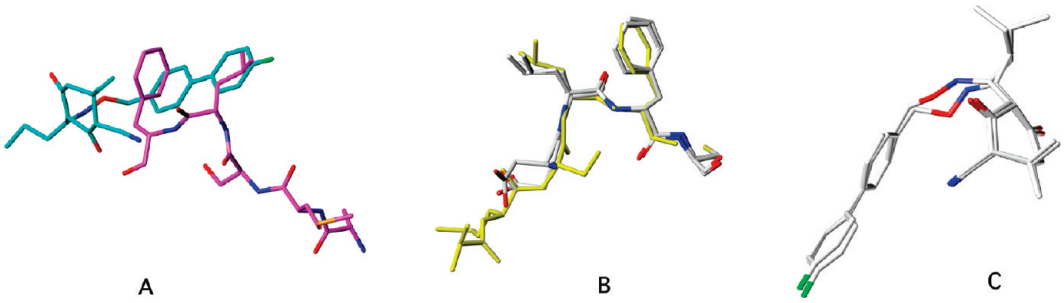

Figure 5. (A) Superimposition of the binding conformation and orientation of ligand **4** (in cyan) and the AMSLF peptide (in magenta; from the $\delta-\beta$ structure, PDB ID: 1JQL[26]) from the X-ray structures of β complexes. Note the close proximity of the L and F side chains of the peptide with the hydrophobic biphenyl moiety in **4**. (B) Superimposition of the X-ray conformation of the AMSLF peptide (in yellow; PDB ID 1JQL[26]) with two DLF conformers from the PDB (in gray) close to the consensus conformation for SLF used for the virtual screen 3D pharmacophore query. (C) Superimposition of different X-ray conformations of **4** from the two binding sites in β_2. The cyclohexanedione and biphenyl rings align well, but the oxime and propyl chains adopt alternate conformations.

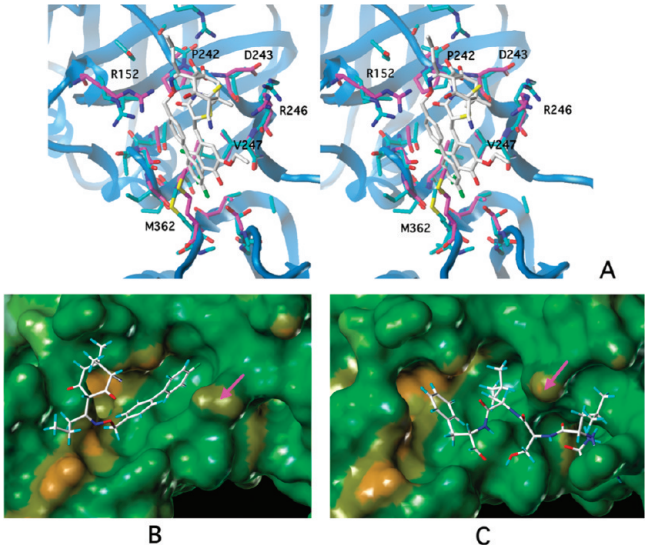

Figure 6. Orientation of ligands in the protein binding pocket of the β_2 sliding clamp from X-ray structures. (A) Stereo view of the $\beta-$**4** and $\beta-$**1** (PDB ID: 3D1G) complexes, with β shown in cartoon form and the compounds in gray sticks. Side-chains of β that interact with **4** have magenta carbon atoms, and those that interact with **1** have cyan carbon atoms. (B) Biphenyloxime ether ligand **4**. (C) AMSLF ligand (PDB ID: 1JQL). The protein is shown as a molecular surface encoded for lipophilicity, with brown indicating hydrophobic and blue indicating hydrophilic regions. The magenta arrows denote the positions of Met362.

compounds are approximately coplanar, but the bulky bromine atoms cause the aromatic ring of **1** to be pushed out of the binding site by about 1.4 Å compared with that of **4** (Figure 6A). The remaining portions of each ligand have little in common. The guanidinium group of Arg152 is in an adjusted position so as to form a hydrogen bond with **1**. Furthermore, the carboxylate moiety of **1** forms a hydrogen bond with the backbone amide of Asp243. Overall, the biphenyl group in **4** makes more hydrophobic contacts, whereas **1** has more hydrogen bonding interactions.

Insights for Improved Ligand Design. The β_2-**4** cocrystal structure identifies important interactions between the fluorobiphenyl moiety and subsite 1 of β. However, inspection of the structure shows that there are several other residues near the ligand that could be accessed by suitable substituents. Thr172 lies approximately 2.5 Å from the 2 positions on both phenyl groups and could interact with a small hydrogen bond acceptor like a fluoro substituent, or form a new hydrogen bond following conversion of one of the phenyl rings to a pyridine. The former strategy may be more effective, as it retains the hydrophobic character of the ligand, and a pyridyl substituent may cause the biphenyl group to rotate by 180° so that the more hydrophilic edge is exposed to the solvent.

Met362 and Ser346 both occupy positions above the distal end of the hydrophobic pocket. A methyl substituent on the 2 position of the distal phenyl ring could make hydrophobic contact with Met362. A small hydrophobic substituent would be required in this position both to prevent twisting of the phenyl rings and because of the short distance (3.5 Å) between the *S*-methyl group of Met362 and the phenyl ring. Ser346 could form a favorable interaction if a hydrogen bond acceptor was placed in the 3 position of the distal phenyl ring or the fluorine was replaced with a better hydrogen bond acceptor. The distance between the 3 and 4 carbon atoms of **4** and the Ser hydroxyl oxygen is 5.3 and 5.0 Å, respectively.

Arg152 is 3.8 Å from the methylene group connecting the oxime to the biphenyl moiety of **4** and 6−7 Å from the C1 atom of the propyl side chain. Both of these methylene carbons could be substituted by hydrogen bond acceptors or acidic groups to create stronger hydrogen bond or salt bridge interactions with this residue. Similarly, Tyr154 is 4−6 Å from this methylene group and the relatively mobile propyl side chain carbons; therefore, decoration of these with hydrogen bond acceptors could lead to enhanced binding. Furthermore, extension of the propyl chain culminating in a hydrogen bond acceptor could access favorable interaction with Tyr153 at the end of this pocket.

In the X-ray structure, Arg246 is quite close to the end of the cyclohexanedione ring, but faces away from the ligand. This residue seems to be relatively mobile; therefore, a suitable hydrogen bond acceptor attached to the equatorial methyl group at the end of the cyclohexane ring may allow Arg246 to swing around and make a hydrogen bond or salt bridge interaction with the ligand.

Comparison of the structure of the bound AMSLF peptide from the structure of the $\beta-\delta$ (clamp loader) complex[26] with that of **4** reveals that the two ligands only partially overlap (Figures 5A and 6B,C), but the binding site retains a very similar structure. Satisfyingly, the conformation of the SLF moiety of the

dx.doi.org/10.1021/jm2004333 |*J. Med. Chem.* 2011, 54, 4831–4838

CBM in the $\beta-\delta$ structure closely resembles the consensus structure for one of its two conserved conformations from the PDB 3D motif search (Figure 5B). The conserved LF residues from the bioinformatics analysis and the biphenyl functional group in **4** selected by the 3D pharmacophore search also bind in the same region of the protein (Figures 5A and 6B,C). However, the small section at the edge of the hydrophobic pocket into which the LF and biphenyl moieties bind changes shape as the ligand is changed. This primarily involves rotation of Met362 (arrows in Figure 6B,C). When the peptide binds, Met362 (arrow in Figure 6C) swings aside to open up a channel in the side of the hydrophobic pocket through which the peptide backbone can pass. When the biphenyl ligand binds, Met362 rotates to be near His175, closing off this channel (Figure 6B). A deeper pocket on the side of the hydrophobic cleft (Figure 6) is occupied by Phe but not by **4**, and placement of a hydrophobic group on the 3 position of the proximal biphenyl ring may enhance binding at this end of the molecule.

These alterations address improvement in binding to the intermolecular binding site on β, but additional modifications would also be required to optimize ADME properties for delivery and bacterial uptake *in vivo*. In particular, the ClogP of **4** is probably too high, and polar groups would need to be introduced to bring it within the ideal range.

CONCLUSIONS

Studies by several groups have shown that the interaction site of the β_2 sliding clamp and its polymerase partners is amenable to modulation by small chemical entities. We have chosen a rational design process to identify such entities.

We used simple modifications of the pentapeptide clamp binding motif (CBM) to derive structural information about the binding requirements of the interaction site on β_2 and then prepared an optimized pentapeptide. A 120-fold improvement of the $\alpha-\beta_2$ IC_{50} and 25-fold improvement in the SPR assay was achieved by N-terminal acetylation and chlorine substitution on the Phe ring in position 5 of the pentameric CBM.

A new method was developed for estimating the likely conformation of the DLF motif within the CBM using a consensus of conserved conformations from the PDB. This allowed pharmacophore models to be defined, and these identified lead molecules in a virtual screen. The crystal structure of β_2 with one of the inhibitors bound revealed details of interactions that can be used to improve the activity of these lead compounds by targeted design modifications. The medicinal chemistry and QSAR of these leads will be described in subsequent papers.

Together with the structure of the β_2-**1** complex,[5] the new structural data form a significant basis for the design of new ligands through lead-hopping, isostere replacement, and computer-aided design. These examples should encourage further investment to meet the urgent need for new classes of antibiotics to challenge the rising tide of drug resistance among bacterial pathogens.

EXPERIMENTAL SECTION

Peptide Synthesis. The synthesis of all the peptides is described in Supporting Information. Briefly, the standard Fmoc/*t*Bu protection strategy was used for solid phase peptide synthesis on a 2-chlorotrityl chloride polystyrene resin; some were synthesized in a 96 well format. Acetylation of the pentamer (with and without the chlorine substitutions on the Phe_5 ring) used acetic anhydride and diisopropylethylamine (DIPEA). As derivatization reagents (Table S5, Supporting Information), carboxylic acid chlorides, sulfonyl chlorides, and chloroformates were used directly, with DIPEA added to the resin prior to the addition of the reagent, while carboxylic acids were used together with *O*-(benzotriazol-1-yl)-*N*,*N*,*N*′,*N*′-tetramethyluronium hexafluorophosphate and DIPEA (4 equiv) as standard couplings. The peptides were purified using standard reverse-phase HPLC methods. All peptides were >95% pure by HPLC and mass spectrometric analyses were consistent with the calculated values.

Inhibition Assays. The $\alpha-\beta_2$ plate binding assays were as described.[19] Stock 2.5 or 5 mM solutions of peptides were prepared in methanol, and dilutions were freshly prepared in aqueous buffers. The NCI and in-house library compounds were dissolved in DMSO at 10 mM and then diluted in aqueous buffers. Only soluble compounds proceeded to assay. The SPR assay was as described.[19]

Molecular Modeling. Pharmacophore searching used the Tripos software pages Sybyl 8.0 (Tripos Inc.) and Unity. The biopolymer peptide sequence search facility was used to extract all examples of the LDLF peptide sequence from structures in the PDB and to align them by Cα superimposition in 3D space. Since there were clearly only two preferred conformations, the few outliers were carefully removed. The terminal binding groups of the amino acid side chains were then used as 3D database queries, with suitable variations in the intergroup distances being permitted. The database searches were carried out in Unity using the 3D flexible search option that allows the main low energy conformations of any putative hit structure to be accessed during the search.

To understand the structural basis of observed trends in binding affinities of peptides with β_2 (Table 1), an atomic model of the peptide Ac-QLDL[3,4ClF] bound to β was constructed using the crystal structure[5] of the Pol II peptide (GQLGLF) complex (PDB ID: 3D1E) as the template. After deleting the N-terminal Gly and N-acetylating the Gln, the central Gly was mutated to Asp, selecting an energetically most favorable side-chain rotamer pointing toward the external solvent. The C-terminal Phe was then modified by 3,4-dichloro substitution on the phenyl ring. These modifications were done with InsightII v. 2005 (Accelrys, San Diego, CA). This structure was then energy minimized with Discover v. 2.98 (Accelrys), using the CVFF force field and a distance-dependent dielectric function. During energy minimization, backbone and all heavy atoms of amino acid residues of β not interacting with the peptide were held fixed.

Chemistry. Detailed synthetic procedures and characterization for all new compounds are in Supporting Information. In brief, the oximinodioxo-cyclohexanes and -pyrans were prepared from the corresponding *N*-alkoxyphthalimide by treatment with *N*,*N*-diethylethylene diamine, followed by reaction with the appropriate 2-acyl-1,3-dicarbonyl compound under acidic conditions.

Structural Biology. The β_2 clamp was prepared as described.[25] Crystals were grown by the hanging drop vapor diffusion method. The reservoir contained 1 mL of a solution of 30% PEG400, 0.17 M calcium acetate, and 0.1 M MES at pH 6.5. Hanging drops contained 2 μL of protein (47 mg/mL), 2.5 μL of 2.3 mM **4** in ethanol, and 2 μL of reservoir solution. X-ray data were collected on a MAR345 area detector using Cu−Kα radiation from a Rigaku RU-200 rotating anode X-ray generator and processed with DENZO and SCALEPACK from the HKL package.[27] The model was refined with REFMAC,[28] with model building in O.[29] Figures were prepared with PyMOL (DeLano Scientific; http://pymol.sourceforge.net/).

ASSOCIATED CONTENT

Supporting Information. Details of the synthesis and characterization of peptides, peptide derivatives, and compounds, including a table showing derivatization reagents, data for inhibition by synthetic peptide derivatives of interactions of

β_2 with α and an immobilized peptide (three tables), and data collection and refinement statistics for X-ray crystallography. This material is available free of charge via the Internet at http://pubs.acs.org.

Accession Codes

[+]The atomic coordinates and structure factors of compound **4** in complex with the *E. coli* sliding clamp have been deposited in the Protein Data Bank, www.rcsb.org (PDB code 3QSB).

AUTHOR INFORMATION

Corresponding Author

*CSIRO Livestock industries, Level 7 QBP, 306 Carmody Rd., St. Lucia, Queensland 4067, Australia. Phone: 61 7 3214 2510. Fax: 61 7 3214 2900. E-mail: gene.wijffels@csiro.au.

Present Addresses

[◆]Novo Nordisk A/S, Novo Nordisk Park, DK-2760 Måløv, Denmark.

[¶]Laboratory for Behavioral Genetics, RIKEN Brain Science Institute, Wako, Saitama 351-0198, Japan.

[+]Cephalon Australia, Level 2, 37 Epping Road, Macquarie Park, New South Wales 2113, Australia.

ACKNOWLEDGMENT

This work was supported in part by grants from the Australian Research Council. N.E.D and A.J.O hold Australian Professorial and Future Fellowships, respectively. P.A.J. was a CSIRO Fellow.

ABBREVIATIONS USED

CBM, clamp binding motif; SPR, surface plasmon resonance; NCI, National Cancer Institute; PDB, Protein Data Bank; DIPEA, *N*,*N*-diisopropylethylamine

REFERENCES

(1) Robinson, A.; Brzoska, A. J.; Turner, K. M.; Withers, R.; Harry, E. J.; Lewis, P. J.; Dixon, N. E. Essential biological processes of an emerging pathogen: DNA replication, transcription and cell division in *Acinetobacter* spp. *Microbiol. Mol. Biol. Rev.* **2010**, *74*, 273–297.

(2) Robinson, A.; Causer, R. J.; Dixon, N. E. Architecture and conservation of the bacterial DNA replication machinery, an under-exploited drug target. *Curr. Drug Targets* **2011**in press.

(3) Dallmann, H. G.; Fackelmayer, O. J.; Tomer, G.; Chen, J.; Wiktor-Becker, A.; Ferrara, T.; Pope, C.; Oliveira, M. T.; Burgers, P. M. J.; Kaguni, L. S.; McHenry, C. S. Parallel multiplicative target screening against divergent bacterial replicases: Identification of specific inhibitors with broad spectrum potential. *Biochemistry* **2010**, *49*, 2551–2562.

(4) Daly, J. S.; Giehl, T. J.; Brown, N. C.; Zhi, C.; Wright, G. E.; Ellison, R. T., III. In vitro antimicrobial activities of novel anilinouracils which selectively inhibit DNA polymerase III of Gram-positive bacteria. *Antimicrob. Agents Chemother.* **2000**, *44*, 2217–2221.

(5) Georgescu, R. E.; Yurieva, O.; Kim, S.-S.; Kuriyan, J.; Kong, X.-P.; O'Donnell, M. Structure of a small-molecule inhibitor of a DNA polymerase sliding clamp. *Proc. Natl. Acad. Sci. U.S.A.* **2008**, *105*, 11116–11121.

(6) Guiles, J.; Sun, X.; Critchley, I. A.; Ochsner, U.; Tregay, M.; Stone, K.; Bertino, J.; Green, L.; Sabin, R.; Dean, F.; Dallmann, H. G.; McHenry, C. S.; Janjic, N. Quinazolin-2-ylamino-quinazolin-4-ols as novel non-nucleoside inhibitors of bacterial DNA polymerase III. *Bioorg. Med. Chem. Lett.* **2009**, *19*, 800–802.

(7) Kong, X.-P.; Onrust, R.; O'Donnell, M.; Kuriyan, J. Three-dimensional structure of the β subunit of *E. coli* DNA polymerase III holoenzyme: a sliding DNA clamp. *Cell* **1992**, *69*, 425–437.

(8) Georgescu, R. E.; Kim, S.-S.; Yurieva, O.; Kuriyan, J.; Kong, X.-P.; O'Donnell, M. Structure of a sliding clamp on DNA. *Cell* **2008**, *132*, 43–54.

(9) Stukenberg, P. T.; Studwell-Vaughan, P. S.; O'Donnell, M. Mechanism of the sliding β-clamp of DNA polymerase III holoenzyme. *J. Biol. Chem.* **1991**, *266*, 11328–11334.

(10) Lovett, S. T. Polymerase switching in DNA replication. *Mol. Cell* **2007**, *27*, 523–526.

(11) Langston, L. D.; Indiani, C.; O'Donnell, M. Whither the replisome: emerging perspectives on the dynamic nature of the DNA replication machinery. *Cell Cycle* **2009**, *8*, 2686–2691.

(12) Jeruzalmi, D.; O'Donnell, M.; Kuriyan, J. Clamp loaders and sliding clamps. *Curr. Opin. Struct. Biol.* **2002**, *12*, 217–224.

(13) Kurz, M.; Dalrymple, B.; Wijffels, G.; Kongsuwan, K. Interaction of the sliding clamp β-subunit and Hda, a DnaA-related protein. *J. Bacteriol.* **2004**, *186*, 3508–3515.

(14) López de Saro, F. J.; O'Donnell, M. Interaction of the β sliding clamp with MutS, ligase, and DNA polymerase I. *Proc. Natl. Acad. Sci. U.S.A.* **2001**, *98*, 8376–8380.

(15) Kongsuwan, K.; Josh, P.; Picault, M. J.; Wijffels, G.; Dalrymple, B. The plasmid RK2 replication initiator protein (TrfA) binds to the sliding clamp β subunit of DNA polymerase III: Implication for the toxicity of a peptide derived from the amino-terminal portion of 33-kDa TrfA. *J. Bacteriol.* **2006**, *188*, 5501–5509.

(16) Leu, F. P.; Hingorani, M. M.; Turner, J.; O'Donnell, M. The δ subunit of DNA polymerase III holoenzyme serves as a sliding clamp unloader in *Escherichia coli*. *J. Biol. Chem.* **2000**, *275*, 34609–34618.

(17) Sutton, M. D.; Duzen, J. M.; Maul, R. W. Mutant forms of the *Escherichia coli* β sliding clamp that distinguish between its roles in replication and DNA polymerase V-dependent translesion DNA synthesis *Mol. Microbiol.* **2005**, *55*, 1751–1766.

(18) Dalrymple, B. P.; Kongsuwan, K.; Wijffels, G.; Dixon, N. E.; Jennings, P. A. A universal protein-protein interaction motif in the eubacterial DNA replication and repair systems. *Proc. Natl. Acad. Sci. U.S.A.* **2001**, *98*, 11627–11632.

(19) Wijffels, G.; Dalrymple, B. P.; Prosselkov, P.; Kongsuwan, K.; Epa, V. C.; Lilley, P. E.; Jergic, S.; Buchardt, J.; Brown, S. E.; Alewood, P. F.; Jennings, P. A.; Dixon, N. E. Inhibition of protein interactions with the β_2 sliding clamp of *Escherichia coli* DNA polymerase III by peptides from β_2-binding proteins. *Biochemistry* **2004**, *43*, 5661–5671.

(20) Dohrmann, P. R.; McHenry, C. S. A bipartite polymerase-processivity factor interaction: Only the internal β binding site of the α subunit is required for processive replication by the DNA polymerase III holoenzyme. *J. Mol. Biol.* **2005**, *350*, 228–239.

(21) López de Saro, F. J.; Georgescu, R. E.; O'Donnell, M. A peptide switch regulates DNA polymerase processivity. *Proc. Natl. Acad. Sci. U.S.A.* **2003**, *100*, 14689–14694.

(22) Bunting, K. A.; Roe, S. M.; Pearl, L. H. Structural basis for recruitment of translesion DNA polymerase Pol IV/DinB to the β-clamp. *EMBO J.* **2003**, *22*, 5883–5892.

(23) Burnouf, D. Y.; Olieric, V.; Wagner, J.; Fujii, S.; Reinbolt, J.; Fuchs, R. P. P.; Dumas, P. Structural and biochemical analysis of sliding clamp/ligand interactions suggest a competition between replicative and translesion DNA polymerases. *J. Mol. Biol.* **2004**, *335*, 1187–1197.

(24) Ihlenfeldt, W.-D.; Voigt, J. H.; Bienfait, B.; Oellien, F.; Nicklaus, M. C. Enhanced CACTVS browser of the open NCI database. *J. Chem. Inf. Comput. Sci.* **2002**, *42*, 46–57.

(25) Oakley, A. J.; Prosselkov, P.; Wijffels, G.; Beck, J. L.; Wilce, M. C. J.; Dixon, N. E. Flexibility revealed by the 1.85 Å crystal structure of the β sliding-clamp subunit of *Escherichia coli* DNA polymerase III. *Acta Crystallogr., Sect. D* **2003**, *59*, 1192–1199.

(26) Jeruzalmi, D.; Yurieva, O.; Zhao, Y.; Young, M.; Stewart, J.; Hingorani, M.; O'Donnell, M.; Kuriyan, J. Mechanism of processivity clamp opening by the delta subunit wrench of the clamp loader complex of *E. coli* DNA polymerase III. *Cell* **2001**, *106*, 417–428.

(27) Otwinowski, Z.; Minor, W. Processing of X-ray diffraction data collected in oscillation mode. *Methods Enzymol.* **1997**, *276*, 307–326.

(28) Murshudov, G. N.; Vagin, A. A.; Lebedev, A.; Wilson, K. S.; Dodson, E. J. Efficient anisotropic refinement of macromolecular structures using FFT. *Acta Crystallogr., Sect. D* **1999**, *55*, 247–255.

(29) Jones, T. A.; Zou, J. Y.; Cowan, S. W.; Kjeldgaard, M. Improved methods for building protein models in electron-density maps and the location of errors in these models. *Acta Crystallogr., Sect. A* **1991**, *47*, 110–119.